

The divergence of flowering time modulated by FT/TFL1 is independent to their interaction and binding activities

Zhen Wang¹, Ruiguang Yang¹, Upendra K. Devisetty², Julin N. Maloof³, Yang Zuo¹, Jingjing Li¹, Yuxiao Shen¹, Jian Zhao⁴, Manzhu Bao¹, Guogui Ning^{1*}

¹College of Horticulture and Forestry Sciences, Huazhong Agricultural University, China,

²BIO5 Institute, University of Arizona, USA, ³Department of Plant Biology, University of California, Davis, USA, ⁴College of Plant Science & Technology, Huazhong Agricultural University, China

Submitted to Journal:
Frontiers in Plant Science

Specialty Section:
Crop Science and Horticulture

ISSN:
1664-462X

Article type:
Original Research Article

Received on:
06 Feb 2017

Accepted on:
18 Apr 2017

Provisional PDF published on:
21 Apr 2017

Frontiers website link:
www.frontiersin.org

Citation:
Wang Z, Yang R, Devisetty UK, Maloof JN, Zuo Y, Li J, Shen Y, Zhao J, Bao M and Ning G(2017) The divergence of flowering time modulated by FT/TFL1 is independent to their interaction and binding activities. *Front. Plant Sci.* 8:697. doi:10.3389/fpls.2017.00697

Copyright statement:
© 2017 Wang, Yang, Devisetty, Maloof, Zuo, Li, Shen, Zhao, Bao and Ning. This is an open-access article distributed under the terms of the [Creative Commons Attribution License \(CC BY\)](#). The use, distribution and reproduction in other forums is permitted, provided the original author(s) or licensor are credited and that the original publication in this journal is cited, in accordance with accepted academic practice. No use, distribution or reproduction is permitted which does not comply with these terms.

This Provisional PDF corresponds to the article as it appeared upon acceptance, after peer-review. Fully formatted PDF and full text (HTML) versions will be made available soon.

Provisional

1
2
3
4

5 **The divergence of flowering time modulated by *FT/TFL1* is** 6 **independent to their interaction and binding activities**

7
8

9 *Zhen Wang¹, Ruiguang Yang¹, Upendra Kumar Devisetty², Julin N. Maloof³, Yang Zuo¹,*
10 *Jingjing Li¹, Yuxiao Shen¹, Jian Zhao⁴, Manzhu Bao¹, Guogui Ning*¹*

11
12 ¹Key laboratory of Horticultural Plant Biology, Ministry of Education, College of Horticulture
13 and Forestry Sciences, Huazhong Agricultural University, Wuhan, P. R. China

14 ²BIO5 Institute, University of Arizona, Tucson, Arizona, United States

15 ³Department of Plant Biology, University of California, Davis, Davis, California, United
16 States

17 ⁴National key laboratory of Crop Genetics and Improvement, College of Plant Science &
18 Technology, Huazhong Agricultural University, Wuhan, P. R. China

19
20 *Correspondence:

21 Prof. Guogui Ning

22 Huazhong Agricultural University

23 College of Horticulture and Forestry Sciences

24 Key laboratory of Horticultural Plant Biology, Ministry of Education

25 No.1, Shizishan Street

26 Wuhan 430070, P. R. China

27 ggning@mail.hzau.edu.cn

28

29

30

31

32

33

34

35

36 **Abstract**

37 FLOWERING LOCUS T (*FT*) and TERMINAL FLOWER1 (*TFL1*) proteins share highly
38 conserved amino acid residues but they play opposite regulatory roles in promoting and
39 repressing the flowering response, respectively. Previous substitution models and functional
40 analysis have identified several key amino acid residues which are critical for the promotion
41 of flowering. However, the precise relationship between naturally occurring *FT/TFL1*
42 homologs and the mechanism of their role in flowering is still unclear. In this study, *FT/TFL1*
43 homologs from eight Rosaceae species, namely, *Spiraea cantoniensis*, *Pyracantha*
44 *fortuneana*, *Photinia serrulata*, *Fragaria ananassa*, *Rosa hybrida*, *Prunus mume*, *Prunus*
45 *persica* and *Prunus yedoensis*, were isolated. Three of these homologs were further
46 characterized by functional analyses involving site-directed mutagenesis. The results showed
47 that these *FT/TFL1* homologs might have diverse functions despite sharing a high similarity
48 of sequences or crystal structures. Functional analyses were conducted for the key FT amino
49 acids, Tyr-85 and Gln-140. It revealed that *TFL1* homologs cannot promote flowering simply
50 by substitution with key *FT* amino acid residues. Mutations of the IYN triplet motif within
51 segment C of exon 4 can prevent the *FT* homolog from promoting the flowering.
52 Furthermore, physical interaction of *FT* homologous or mutated proteins with the
53 transcription factor FD, together with their lipid-binding properties analysis, showed that it
54 was not sufficient to trigger flowering. Thus, our findings revealed that the divergence of
55 flowering time modulating by *FT/TFL1* homologs is independent to interaction and binding
56 activities.

57 **Key words:** *FT/TFL1* homologs, site mutated, transgenic research, protein interactions, binding activity,
58 Rosaceae species

59

60 **Introduction**

61 Flowering is a key developmental phase of the higher plants. The transition from the
62 vegetative to reproductive growth phase is tightly regulated by a complex arrangement of
63 multiple signaling networks. In *Arabidopsis thaliana*, multiple regulatory pathways involved
64 in the flowering have been thoroughly researched. Generally it includes photoperiod,
65 vernalization, hormone, autonomous and age-dependent pathways (Mutasa-Göttgens and
66 Hedden, 2009; Wang et al., 2011a; Turnbull, 2011; Johansson and Staiger, 2015; Wagner,
67 2016). These multiple pathways converge upon a small set of key flowering time genes which
68 are responsible for growth phase transition and the onset of flowering. The mobile florigen
69 *FLOWERING LOCUS T (FT)*, *SUPPRESSOR OF OVEREXPRESSION OF CONSTANS1*
70 (*SOC1*) and *LEAFY (LFY)* genes function as integrators of different regulatory pathways.

71 *FT* and *FT*-homologs are floral promoter genes and they are highly conserved in a wide
72 range of plant species (Coelho et al., 2014; Xing et al., 2014; Wolabu et al., 2016). Current
73 understanding is that the *FT* gene is expressed within the leaves, while the mature protein
74 moves to the shoot apex via the phloem, where it interacts with FD to participate in the
75 promotion of flowering (Wigge et al., 2005; Notaguchi et al., 2008; Benlloch et al., 2011).
76 Thus, *FT* had been extensively studied as a candidate for the mobile flower-promoting signal
77 known as “florigen” (Kobayashi and Weigel, 2007; Corbesier et al., 2007; Tamaki et al.,
78 2007). Conversely, flowering is strongly repressed by the *FT* homolog, *TFL1* (Bradley et al.,
79 1997; Ohshima et al., 1997). In *Arabidopsis*, *TFL1* has been proposed to repress flowering
80 both by antagonizing the activity of *FT* and also through an independent flowering control
81 activity (Kardailsky et al., 1999; Kobayashi et al., 1999; Pnueli et al., 2001).

82 *FT* and *TFL1* encode proteins approximately 175 amino acids and their structure is
83 similar to a phosphatidylethanolamine-binding protein (PEBP) family found in mammalian,
84 yeast and bacteria (Grandy et al., 1990; Bradley et al., 1996). PEBPs have been shown to act
85 in multiple roles as modulators in cell growth and differentiation (Hengst et al., 2001; Fu et
86 al., 2003; Chautard et al., 2004). Plant PEBP-related genes were initially cloned from
87 *Antirrhinum* (Bradley et al., 1996), *Arabidopsis* (Bradley et al., 1997) and tomato (Pnueli et
88 al., 1998). The structure of each of these proteins have now also been illustrated (Banfield and
89 Brady, 2000; Ahn et al., 2006). It revealed that the tertiary structures of the plant PEBPs are
90 also closely similar to those of animal counterparts, being dominated by a large central β -
91 sheet with an anion binding pocket contacted by a C-terminal peptide. However, there is no
92 direct evidence in the plant PEBPs that phospholipids or other anions binding to this pocket *in*
93 *vivo*, as seen in the animal PEBPs (Banfield et al., 1998; Serre et al., 1998; Simister et al.,
94 2002). The phospholipid binding activity test showed that FT bound to the lipid
95 phosphatidylcholine (PC) *in vitro*, but not to phosphatidylethanolamine (PE). It was partially
96 related to FT activity since the ratio of PC: PE increasing accelerates flowering (Nakamura et
97 al., 2014).

98 FT and TFL1 play opposing roles in the control of flowering, though there are only 39
99 non-conservative residues between them in *Arabidopsis* (Ho and Weigel, 2014). Thus, the
100 question is arisen whether certain critical residues are responsible for the diversity of their
101 functions. It has been reported that Tyr-85 in FT and His-88 in TFL1 play key roles in their
102 respective functions. Substitution of the amino acid residues at these positions (i.e. replacing
103 Tyr to His in FT, or His to Tyr in TFL1) was found to confer partial TFL1-like activity on the
104 altered FT protein and weak FT-like activity on the altered form of TFL1 (Hanzawa et al.,
105 2005). *Arabidopsis* demonstrated an early flowering phenotype when an *OnTFL1* orchid
106 homologue H85Y was ectopically expressed (Hou and Yang, 2009). Subsequent experiments
107 showed an external loop structure (residues 128-145), together with the adjacent peptide
108 segment, contributed to the opposite FT and TFL1 activities (Ahn et al., 2006). The external
109 loop segment is almost invariant in FT orthologs, but it seems to have evolved rapidly in
110 TFL1 orthologs. Furthermore, a specific residue in this external loop structure makes a
111 hydrogen bond with His-88 near to the entrance of a potential ligand-binding pocket in TFL1,
112 but not in FT (Hanzawa et al., 2005; Ahn et al., 2006; Ho and Weigel, 2014). In sugar beet
113 (*Beta vulgaris* subsp. *vulgaris*), two paralogs of *FT* (i.e. *BvFT1* and *BvFT2*) both contain Tyr-
114 85 and Gln-140, but they have naturally evolved antagonistic functions. Whereas *BvFT2* is
115 essential for flowering, *BvFT1* acts as a flowering repressor. In *BvFT1* it was shown that the
116 alteration of three amino acids in the external loop structure could reverse its repressor
117 function into a floral promotion role (Pin et al., 2010). Ho and Weigel (2014) found that
118 specific mutations at the four Glu-109, Trp-138, Gln-140 and Asn-152 residues could
119 transform FT into a TFL1-like floral repressor.

120 Here, we report the isolation and characterization of the *FT/TFL1* homologs of eight
121 Rosaceae species. Ectopic overexpression analysis of various *FT/TFL1* homologs showed that
122 there was a diversity function among them in spite of the high levels of similarity. Site
123 mutation analysis of selected *FT/TFL1* homologs identified a specific amino acid residue (N-
124 154 of RoFT), not previously reported, to be important to the maintenance of floral
125 promoting. Interaction analysis between AtFD and the phenotype specific *FT/TFL1* homologs
126 or mutations indicated that FT homologs in flowering promotion are not a simple function of
127 the interaction with FD. In addition, the putative phospholipid binding investigations shown
128 that all of flowering promoted or delayed *FT/TFL1* homologs or mutations have the same
129 lipid-binding properties. Our findings provide evidence that the diversity of flowering time
130 modulating by *FT/TFL1* homologs is independent to their interaction and binding activities.

131

132 Materials and methods

133 Plant materials

134 Plants of eight Rosaceae species were from the experimental plots at Huazhong Agricultural
135 University, Wuhan, P.R. China. *Nicotiana tabacum* cultivar 'Xanthi', *Arabidopsis thaliana*
136 Col and *ft-1* *Arabidopsis* mutant (Ler ecotype) were used for wild controls.

137 Molecular cloning and phylogenetic analysis of FT/TFL1 homologs

138 Genomic DNA from eight Rosaceae species was extracted from young leaves as described
139 previously by Wang et al. (2011). Total RNA was extracted according to a previous protocol
140 (Hu et al., 2002). The initial *FT/TFL1* genomic DNA sequences were isolated by homology
141 cloning strategies and genome walking methods (Wang et al., 2011). The degenerated primers
142 were designed according to the *FT/TFL1* sequences from other Rosaceae species. For cloning
143 of the *FT* homologs, the degenerated primers used were: FTF1, 5'-
144 ATGCCTAGGAHAGGGAYCCYCTTGTT-3', FTF2, 5'-
145 GCAACAAACGGCGGCAAGCTT-3', and FTR, 5'-
146 CCAGAGCCRCYCTCCCTYTGGCAGTT-3'. For cloning of the *TFL1* homologs, the
147 degenerated primers used were: TFL1F, 5'- TTGGNAGAGTGATAGGAGATGTT-3',
148 TFL1R, 5'-GAGGAAGGTGKGTGATTGA-3'. Fusion primer and nested integrated PCR
149 (FPNI-PCR) was used to isolate the unknown sequences flanking the core sequences
150 amplified from the degenerated primers. The full-length *FT/TFL1* cDNA sequence was
151 isolated by specific primers (Supplementary Tables S1-S3). Amino acid sequences were
152 aligned using CLUSTALW MULTIPLE ALIGNMENT with default parameters. Phylogenetic
153 studies were performed using MEGA5 based on the neighbor-joining method (Tamura et al.,
154 2011). Nodal support was estimated by bootstrap analysis and an interior branch test on the
155 basis of 1000 re-samplings.

156 Structure determination

157 Protein structures of FT and TFL1 homologs were obtained using SWISS-MODEL workspace
158 (Arnold et al., 2006; <http://swissmodel.expasy.org>) and visualized by UCSF Chimera
159 (Pettersen et al., 2004). The three-dimensional structures of 3AXY and 1WKO were used as
160 loading template for FT and TFL1, respectively.

161 Site-directed mutagenesis of known *FT/TFL1*

162 The gene splicing overlap extension PCR method (SOE-PCR) (Ho et al., 1989) was used to
163 get a pre-determined point mutagenic site in *FT/TFL1* sequences. We designed a pair of
164 complementary oligo primers in which 1 or 2 base pairs had been altered to introduce a
165 specific mutation into the amplified gene sequence. These mismatch primers mutants (i.e.
166 RoFTmu1F & RoFTmu1R) were paired with unaltered RoFTR and RoFTF primers,
167 respectively, and were used for PCR to generate two DNA fragments with overlapping ends.
168 The two fragments were combined in a subsequent 'fusion' reaction PCR using RoFTF and
169 RoFTR primers (Supplementary Table S4). All point mutagenic sequences were introduced
170 into pMD18-T and then pMOG22 vector (Mogen, Leiden, The Netherlands).

171 Plasmid construction and plant transformation

172 The *RoFT*, *RoTFL1*, *FaTFL1*, *PhFT* and *AtFD* genes were amplified by PCR from each RNA
173 with the appropriate specific primers (Supplementary Table S4). The amplified products were
174 cloned into pMD18-T vector (Takara) and sequenced. Then the inserts were subcloned into

175 the modified binary vector pMOG22 containing the cauliflower mosaic virus (CaMV) 35S
176 promoter and the Nos terminator.

177 For *Arabidopsis* transformation, the constructs in binary vectors were introduced into
178 *Agrobacterium tumefaciens* strain GV3101. Transgenic plants were generated by floral dip
179 method and the T1 transformants were selected on hygromycin plates for 1 week in LD (16-h-
180 light/8-h-dark) and then transferred to soil at 20-24°C under long day condition (16-h-light/8-
181 h-dark).

182 Tobacco was transformed by *Agrobacterium tumefaciens* strain EHA105 according to
183 previously described method (Ning et al., 2012). All transgenic tobacco plants were kept in
184 the greenhouse under a photoperiod of 12-h-light/ 12-h-dark. Data were collected from at
185 least 20 individuals and evaluated by analysis of variance (one-way ANOVA). Means were
186 compared using Duncan's multiple range test.

187 **qRT-PCR analysis**

188 For real time qRT-PCR analysis, samples were harvested from the shoot apex of 45-day-old
189 seedlings of T1 transgenic tobacco plants or 3-week-old seedlings of transgenic *Arabidopsis*
190 plants. Three biological replications were performed randomly for each transgenic line. Total
191 RNA was isolated using Trizol reagent (Takara) according to the manufacturer's instructions.
192 The first strand of cDNA was synthesized using 2 µg of total RNA as a template with the
193 TransScript™ one-step gDNA Removal and cDNA Synthesis Supermix (Transgen, Beijing,
194 China). The qRT-PCR was performed on 7500 Fast Real-Time PCR System (Applied
195 Biosystems) with SYBR® Premix EX Tag™ (Takara). The tobacco *NtEF1α* and *Arabidopsis*
196 *AtEF1α* transcript were used as an internal standard to calculate the relative expression by the
197 comparative CT ($\Delta\Delta CT$) method, respectively. The primers for RT-PCR and qRT-PCR are
198 detailed in Supplementary Table S5 and S6.

199 **Yeast two-hybrid analysis**

200 The coding sequences of *AtTFL1*, *RoFT*, *RoFTmu1/2/3/4/5*, *FaTFL1*, *RoTFL1* and *PhFT* (all
201 containing the EcoR1 and Sal1 restriction sites at the 5' and 3' ends, respectively) were cloned
202 into bait plasmid PGBKT7. *Arabidopsis FT* (*AtFT*) was also introduced to the PGBKT7
203 plasmid, using the Nde1 and Sal1 restriction sites, as a positive control. The full-length
204 *Arabidopsis FD* coding sequence (*AtFD*) was cloned into prey plasmid PGADT7 using the
205 Nde1 and BamH1 restriction sites. Yeast cells were transformed using Frozen-EZ Yeast
206 Transformation II™ kit (ZYMO RESEARCH, USA). Co-transformed yeast cells were
207 selected on SD-Leu/-Trp plates. Interactions were tested on SD-Leu/-Trp/-His/-Ade/X-a-Gal
208 selective media. Three independent clones for each transformation were tested.

209 **Bimolecular fluorescent complementation (BiFC) analysis**

210 Strain of *Agrobacterium tumefaciens* GV3101 carrying the BiFC constructs were used for the
211 infiltration of 5-6-week-old *N. benthamiana* leaves, according to the protocol described by Li
212 (2015). Of which, the coding sequences of *AtFT*, *AtTFL1*, *RoFT*, *RoFTmu1/2/3/4/5*, *FaTFL1*,
213 *RoTFL1* and *PhFT* were introduced into the vector pFGC-YC155, respectively. The *AtFD*
214 coding sequence was cloned into the vector pFGC-YN173. All vectors were constructed by
215 Gibson assembly method (Gibson et al., 2009). The primers are detailed in Supplementary
216 Table S7. YFP fluorescence was visualized by confocal laser scanning microscope (LSM510
217 Meta, Zeiss, Germany).

218 **Expression and purification of His-tagged FT protein**

219 The coding sequences of *AtFT*, *RoFT*, *RoFTmu2/3/4/5*, *PhFT*, *AtTFL1*, *RoTFL1*, and *FaTFL1*
220 were amplified with the primers which were used to construct PGBK7 vectors before
221 (Supplementary Table S7), and finally cloned into the EcoR1/Sal1 (Sac1/Sal1 for *AtFT*) sites
222 of PET-32a vector (NOVAGEN) to obtain PET32a-His-FT. The ten PET32a-His-FT plasmids
223 were transformed into competent *E. coli* Rosetta (DE3) cells (Transgen, Beijing, China).
224 Fusion protein expression was induced at an OD₆₀₀ of about 0.5 by adding IPTG (isopropyl β-
225 D-1-thiogalactopyranoside) (0.2mM final concentration), in which the cells were grown
226 overnight and the temperature was shifted from 37°C to 16°C. The expressed soluble proteins
227 were purified with Ni-Agarose (CWBIO, Beijing, China) according to the manufacturer's
228 instructions.

229 **Fat Western Blotting**

230 18:1-PC (1, 2-Dioleoyl-sn-Glycero-3-phosphatidylcholine) standards was purchased from
231 Larodan (Sweden). The reaction was performed according to the modified protocol described
232 by Stevenson (1998). Of which, a goat anti-rabbit IgG conjugated to alkaline phosphatase
233 (CWBIO, Beijing, China) against 6X histidine was diluted at a 1:10000 level, and the protein
234 bound to the lipid spot was detected by alkaline phosphatase substrate according to the
235 manufacturer's instructions (Promega).

236 **Accession Numbers**

237 Sequence data from this article can be found in NCBI under the following accession numbers:
238 *Arabidopsis* AtFT (AF152096); *Beta* BvFT1 (HM448910); *Beta* BvFT2 (HM448912); *Citrus*
239 CiFT (AB027456); *Fragaria* FaFT (CBY25183); *Malus* MdFT1 (BAD08340); *Malus* MdFT2
240 (ADP69290); *Nicotiana* NtFT1 (JX679067); *Nicotiana* NtFT2 (JX679068); *Nicotiana* NtFT3
241 (JX679069); *Nicotiana* NtFT4 (JX679070); *Oncidium* OnFT (ACC59806); *Oryza* Hd3a
242 (AB052944); *Petunia* PhFT (ADF42571); *Photinia* PsFT (AEO72028); *Platanus* PaFT
243 (ACX34055); *Populus* PnFT1 (AB106111); *Populus* PnFT2 (AB109804); *Populus* PnFT3
244 (AB110612); *Prunus mume* PmFT (CBY25181); *Prunus persica* PpFT (AEO72030);
245 *Pyracantha* PfFT (AEO72029); *Pyrus pyrifolia* PpFT (KF240775); *Rosa* RoFT (CBY25182);
246 *Spiraea* ScFT (AEO72031); *Vitis* VvFT (ABF56526); *Zea* ZmFT (ABW96237);
247 *Arabidopsis* TFL1 (U77674); *Antirrhinum* CEN (CAC21564); *Citrus* CiTFL1 (AY344245);
248 *Fragaria* FaTFL1 (AEO72027); *Malus* MdTFL1-1 (AB162040); *Malus* MdTFL1-2
249 (AB366643); *Oryza* FDR1 (AF159883); *Oryza* FDR2 (AF159882); *Photinia* PsTFL1
250 (AEO72024); *Populus* PnTFL1 (AB181183); *Prunus mume* PmTFL1 (AEO72021); *Prunus*
251 *persica* PpTFL1 (ADL62867); *Prunus yedoensis* PyTFL1 (AEO72023); *Pyracantha* PfTFL1
252 (AEO72026); *Pyrus pyrifolia* PpTFL1-1 (BAD10962); *Pyrus pyrifolia* PpTFL1-2
253 (BAK74839); *Rosa* RoTFL1 (AEO72022); *Spiraea* ScTFL1 (AEO72025); *Vitis* VvTFL1
254 (AF378127); *Zea* ZmTFL1 (ABI98712).

255

256 **Results**

257 **FT/TFL1 similarity analysis in Rosaceae species**

258 *FT/TFL1* orthologs of eight Rosaceae species, namely, *Spiraea cantoniensis*, *Pyracantha*
259 *fortuneana*, *Photinia serrulata*, *Fragaria ananassa*, *Rosa hybrida*, *Prunus mume*, *Prunus*
260 *persica* (only for *FT*) and *Prunus yedoensis* (only for *TFL1*), were isolated. Two *TFL1* copies
261 were isolated from *Fragaria ananassa* genomic DNA, but only one gene copy was isolated
262 from all other genotypes. Each of the isolated *FT/TFL1* sequences contained four exons and
263 three introns. In all isolated genes, the sizes of the second and third exons were the same, i.e.

62 bp and 41 bp, respectively (**Figure 1A, B**). The seven *FT/TFL1* sequences share 92.09% and 90.59% identity, respectively (Supplementary Figure S1). All *FT/TFL1* homologs from the eight Rosaceae species were found to contain the (putative) crucial amino acid residues of Tyr-85 (for FT) and His-88 (for TFL1). Based on the construction of the phylogenetic tree, it was deduced that all seven *FT* orthologs were clustered within the *FT*-like group and all seven *TFL1* orthologs were clustered within the *TFL1*-like group (**Figure 1C**).

Functional determination of the *FT/TFL1* homologs of Rosaceae species

For functional study of *FT/TFL1* homologs from eight Rosaceae species, we constructed over-expression vectors harboring *FT* and *TFL1* homologs (cDNA) of *Prunus mume*, *Rosa hybrida* and *Fragaria ananassa*. The three species represent different vegetative growth and flowering habit. Two *TFL1* copies were isolated from *Fragaria ananassa* genomic DNA, namely, *FaTFL1-1* and *FaTFL1-2*. There are three single-base differences between the two predicted CDS regions. But only one copy was amplified from the cDNA which shared the same sequence with the predicted CDS region of *FaTFL1-1* gDNA sequence.

According to the results from twenty independent transgenic tobacco lines, the majority of over-expressing *RoFT* and *PmFT* tobacco lines (**Figure 2A, B**), exhibited strongly advanced flowering traits, this was consistent with an earlier preliminary analysis (Ning et al., 2012). At time of flowering, the wild-type had generated 28.6 ± 1.1 leaves, compared with 6.8 ± 1.0 and 5.9 ± 1.1 leaves in the 35S::*RoFT* lines R0-4 and R0-15, respectively (**Table 1**). In contrast to the strongly advanced flowering of *RoFT* and *PmFT* lines, the over-expression of *FaFT* in line F0-1 produced a moderately late flowering time (almost 30 days later relative to wild-type). The number of leaves and height remained comparable to the wild-type (**Table 1**). One of the transgenic line F0-9's flowering time was approx. 50-days later than the wild-type. Thus, there was clearly some functional divergence with respect to the control of flowering between the *FT* orthologs from the different plant species.

The majority of 35S::*PmTFL1*, 35S::*RoTFL1* and 35S::*FaTFL1* transformants flowered much later than wild-type plants. Most transformants did not flower in less than 7 months after sowing, as compared to approx. 5.5 months seen in wild-type plants. In some extreme cases, flowering in transformed plants was delayed to over 12 months after sowing (**Figure 2H**). As shown in **Table 1**, the two selected lines transformed with 35S::*FaTFL1* had produced as many as over twice leaves on the main stem to wild-type plants by the time of flower initiation. Transformants expressing 35S::*PmTFL1* and 35S::*RoTFL1* showed very similar results to those shown for 35S::*FaTFL1* transgenic lines. Therefore, tobacco plants overexpressing the three *TFL1* orthologs from *Prunus mume*, *Rosa hybrida* and *Fragaria ananassa* had an extended vegetative phase and a strongly delayed transition to the reproductive phase.

A similar phenotype to this late flowering imposed by Rosaceae *TFL1* homologues also resulted from the over-expression of a *FT* homolog which was isolated from *Petunia hybrida* (**Figure 2D, E**). The *PhFT* gene contained the Tyr-85 residue and LYN/IYN triplet motif as typical FT sequences, but a Lys-139 residue replaced the normal amino acid in *FT* (i.e. Gln-140); the corresponding residue in *TFL1* was Asp-144 (Supplementary Figure S2). The resulting 35S::*PhFT* transgenic tobacco reached over 2 m in height because of extremely late flowering. Thus, it demonstrated a new role of *TFL1* although it was identified as an *FT* homolog in our phylogenetic analysis.

308

Table 1. Flowering phenotypes of representative T₁ transgenic tobacco lines harboring various *FT/TFL1* homologs.

genotype	Line label	n	no. leaves on main stem at flowering	plant height at first flower bud (cm)	time from seed to first flower bud (days)
<i>Wt</i>	<i>Wt</i>	10	28.6±1.1e	120.2±3.8f	168.8±6.6h
<i>35S::RoFT</i>	R0-4	20	6.8±1.0f	16.4±2.7g	46.9±4.3ij
	R0-15	20	5.9±1.1f	13.4±2.6gh	41.3±2.6j
<i>35S::PmFT</i>	P0-8	20	5.5±0.9f	10.6±2.8h	42.5±4.9ij
	P0-10	20	6.4±1.1f	11.5±3.0gh	49.0±2.1i
<i>35S::FaFT</i>	F0-1	20	30.5±1.9e	123.4±4.9f	194.6±6.9g
	F0-9	20	38.9±3.1d	130.9±4.4e	218.5±7.8f
<i>35S::PhFT</i>	T0-3	20	69.3±3.8c	174.2±4.4cd	294.0±7.1e
	T0-7	20	77.2±2.9b	180.2±3.5b	320.2±6.8c
<i>35S::RoTFL1</i>	T0-5	20	66.3±3.6c	172.9±4.5d	291.4±10.2e
	T0-8	20	85.1±3.4a	176.6±4.2c	372.8±14.3b
<i>35S::PmTFL1</i>	T0-2	20	68.3±3.1c	173.9±3.2cd	301.0±9.1d
	T0-7	20	79.8±7.3b	185.0±6.5a	385.1±7.9a
<i>35S::FaTFL1</i>	L1	20	65.8±3.3c	174.5±5.0cd	294.9±7.0e
	L2	20	80.1±5.1b	187.1±9.8a	387.9±9.2a

311 Notes: n = number of independent plants analyzed. Values are mean ± SE. Figures followed by common
 312 letters within the same column are not significantly different at P = 0.05.

313

314 Identification of key amino acids regulating the activity of *FT/TFL1* 315 homologs

316 Since *Rosa FT* (*RoFT*) and *Fragaria FT* (*FaFT*) exhibited quite different effects on flowering
 317 time in transgenic tobacco, we compared their sequences in more detail. The two proteins
 318 share approximately 88% identity with 13 non-conserved substitutions amongst 20 different
 319 amino acids (Supplementary Figure S1, S2), to be key in their flowering time function. We
 320 focused on five amino acids, which corresponding to residues 7, 65, 116, 153 and 154 in
 321 *RoFT*. The amino acids at positions 7, 65, 116 and 153 in *RoFT* were changed individually to
 322 correlate with the corresponding amino acid residues encoded by *FaFT* (Figure 3A, B). In
 323 addition, we mutated the amino acid N-154 which is identical between *RoFT* and *FaFT*
 324 within the IYN triplet motif of segment C in exon 4. The five resulting mutants were
 325 respectively named *RoFTmu1-5* and each was over-expressed under the control of the
 326 constitutive CaMV 35S promoter (Figure 3C).

327 Tobacco plants over-expressing *RoFTmu1* (R7Q), *RoFTmu2* (T65I) and *RoFTmu3*
 328 (A116S) displayed an early-flowering phenotype, comparable to the native *RoFT* in
 329 transgenic tobacco. In contrast, *35S::RoFTmu4* (Y153C) and *35S::RoFTmu5* (N154D)
 330 transgenic plants showed a strong late flowering phenotype (Figure 4A). As shown in Table
 331 2, *35S::RoFTmu1*, *35S::RoFTmu2* and *35S::RoFTmu3* tobacco plants flowered after
 332 producing approx. 8 to 10 leaves over 2 months of growth. By contrast, the majority of the
 333 *35S::RoFTmu4* and *35S::RoFTmu5* transformants had a much delayed flowering time,
 334 requiring 210±27.1 and 248.1±32.7 days of growth, respectively. We also ectopically
 335 expressed *35S::Roftmu3* (A116S) and *35S::RoFTmu4* (Y153C) in *Arabidopsis* Col.
 336 *35S::RoFTmu3* (A116S) plants showed a marked early flowering phenotype, with
 337 approximately 50% the number of leaves as found in the wild-type Col at floral initiation
 338 (Figure 5A-C). Transgenic *35S::Roftmu4* (Y153C) *Arabidopsis* flowered slightly later than
 339 the corresponding wild-type Col (Figure 5A-C). In addition, overexpressing *RoFTmu1*,

340 *RoFTmu2* and *RoFTmu3* within *ft-1* mutant (*Ler* ecotype) resulted in significant early
 341 flowering compared to *ft-1* plants (**Figure 5E**). As shown in **Figure 5G**, *ft-1* mutant harboring
 342 *35S::RoFTmu3* possessed 9.1 ± 0.9 rosette leaves at the time of bolting, which is almost
 343 consistent to that resulted from *35S::RoFT* (8.9 ± 0.7), while, *ft-1* mutant had produced as
 344 many as > 3-fold leaves (30.2 ± 2.5) until flowering. Meanwhile, the flowering time was much
 345 earlier than those *ft-1* plants (**Figure 5H**).

346

347 **Table 2.** Flowering phenotypes of regenerated T₀ transgenic tobacco lines harboring mutated
 348 *RoFT* transcripts.

genotype	n	no. leaves on main stem at flowering	plant height at first flower bud (cm)	time between transformed plantlet regeneration and first flower bud (days)
<i>Wt</i>	6	26.7 ± 1.0 c	121.7 ± 4.4 d	160.7 ± 6.6 c
<i>35S::RoFT</i>	20	8.3 ± 0.9 d	18.7 ± 1.9 e	47.6 ± 6.3 d
<i>35S::RoFTmu1</i>	22	9.3 ± 1.1 d	18.6 ± 1.8 e	57.8 ± 8.9 d
<i>35S::RoFTmu2</i>	24	9.3 ± 0.8 d	20.3 ± 2.1 e	53.9 ± 8.8 d
<i>35S::RoFTmu3</i>	22	9.0 ± 1.2 d	20.0 ± 2.1 e	47.3 ± 9.6 d
<i>35S::RoFTmu4</i>	5	26.4 ± 0.5 c	126.0 ± 4.2 cd	152.0 ± 10.4 c
	15	41.7 ± 10.3 b	148.1 ± 11.8 b	210.7 ± 27.1 b
<i>35S::RoFTmu5</i>	3	27.3 ± 0.6 c	129.0 ± 3.6 c	161.7 ± 7.6 c
	17	49.3 ± 10.3 a	161.1 ± 13.0 a	248.1 ± 32.7 a

349 Notes: n = number of independent plants analyzed. Other codes are the same as given in Table 1.
 350

351 It has been reported that the opposite roles of FT and TFL1 are related to the conserved
 352 amino acids His-88 and Asp-144 in TFL1 (Hanzawa et al., 2005; Ahn et al., 2006). To
 353 examine whether these amino acids is also conserved in other plant species, we constructed
 354 mutants *RoTFL1mu1* (H82Y), *RoTFL1mu2* (D137Q), *FaTFL1mu1* (H84Y) and *PhFTmu1*
 355 (K139Q) (**Figure 3B**), and transferred them into tobacco plants. As shown in **Figure 4C** and
 356 **4D**, no early flowering phenotype was observed in any of these transformants, as compared to
 357 wild-type tobacco. In fact, some of these transgenic plants remained in the vegetative growth
 358 phase for over 11 months (**Table 3**).

359

360 **Table 3.** Flowering phenotypes of regenerated T₀ transgenic tobacco lines harboring mutated
 361 *TFL1*-like transcripts.

genotype	n	no. leaves on main stem at flowering	plant height at first flower bud (cm)	time between transformed plantlet regeneration and first flower bud (days)
<i>Wt</i>	5	28.8 ± 1.3 b	125.8 ± 4.1 b	163.4 ± 4.8 b
<i>35S::RoTFL1mu1</i>	2	25.5 ± 0.7 b	116.5 ± 2.1 b	131.5 ± 4.9 b
	19	64.7 ± 10.1 a	170.5 ± 11.0 a	287.9 ± 33.1 a
<i>35S::RoTFL1mu2</i>	2	29.5 ± 0.7 b	129.0 ± 1.4 b	169.0 ± 1.4 b
	19	64.1 ± 12.0 a	169.4 ± 10.4 a	284.5 ± 34.6 a
<i>35S::FaTFL1mu1</i>	4	23.8 ± 0.5 b	119.3 ± 1.0 b	127.5 ± 2.9 b
	16	60.6 ± 11.4 a	164.8 ± 10.2 a	269.4 ± 31.5 a

<i>35S::PhFTmu1</i>	20	63.2±7.8a	172.1±9.2a	286.5±27.5a
---------------------	----	-----------	------------	-------------

362 Note: Codes are the same as given in Tables 1 and 2.

364 Expression of floral genes in specific transgenic plants

365 According to previous studies (Abe et al., 2005; Wigge et al., 2005; Searle et al., 2006), the
 366 FT protein activates the floral meristem identity genes *APETALA1* (*API*), *SOC1* and *LFY*.
 367 These have been identified as important floral pathway integrators in *Arabidopsis*. The
 368 expression of the *LFY*, *API* and *SOC1* orthologs, *NtNFL*, *NtAPI* and *NtSOC1* of tobacco was
 369 evaluated by real-time RT-PCR in the shoot apex of 45-day-old seedlings of T1 transgenic
 370 lines and wild type (Smykal et al., 2007; Zhang et al., 2014). *NtNFL* (**Figure 4G**), *NtAPI*
 371 (**Figure 4H**) and *NtSOC1* (**Figure 4I**) were highly up-regulated in *35S::RoFT*,
 372 *35S::RoFTmu1*, *35S::RoFTmu2* and *35S::RoFTmu3* transgenic tobacco plants, which all
 373 showed an early-flowering phenotype. There was no obvious change in transcript levels of
 374 these endogenous genes in the *35S::RoFTmu4* and *35S::RoFTmu5* transgenic plants, which
 375 showed a late-flowering phenotype. Similarly, the expression of *AtAPI*, one of a downstream
 376 gene of FT, was up-regulated in *35S::RoFTmu3* transgenic *Arabidopsis* plant (**Figure 5D**).

377 Interaction of AtFD with FT/TFL1 homologs

378 According to the literature, both FT and TFL1 can interact with the bZIP transcription factor
 379 FD, which regulates the expression of several flower meristem (FM) identity genes (Abe et
 380 al., 2005; Benloch et al., 2011). In order to examine whether Rosaceae FT/TFL1 homologs
 381 are able to interact with FD, and whether single amino acid substitutions in RoFT can affect
 382 the interaction, we performed yeast two-hybrid assays. *Arabidopsis* FD (AtFD) was used as a
 383 prey, and various FT/TFL1 homologs were cloned as the bait. Transformed yeast cells
 384 growing on SD/-Leu-Trp selection medium were shown in Supplementary Figure S3. The
 385 results indicated that in yeast, AtFD was able to interact with AtFT, RoFT and five RoFTmu1-
 386 5 point-mutated forms. However, no interaction was observed of AtFD with AtTFL1,
 387 FaTFL1, RoTFL1 or PhFT. (**Figure 6A**). To further verify the interaction of FT/TFL1
 388 homologs and AtFD, the N-terminal half of YFP fused to AtFD (AtFD-YFP^N) and the C-
 389 terminal half of YFP fused to FT (FT-YFP^C) were employed to perform BiFC test. YFP
 390 fluorescence was obviously observed in the nucleus (**Figure 6B**). The two results indicated
 391 that, except FaTFL1 and RoTFL1, the other FT/TFL1 homologs were able to interact with
 392 AtFD in the nucleus.

393 PC binding activities *in vitro*

394 To test whether RoFT, point mutated RoFT and PhFT have the lipid-binding property, we
 395 performed a Fat-Western blotting using membrane-lipid overlay assays. All of the AtFT,
 396 RoFT, RoFTmu2/3/4/5 PhFT, AtTFL1, RoTFL1 and FaTFL1, with a C-terminal histidine tag,
 397 were expressed and purified (**Figure 7A**). The fusion proteins were hybridized with PC-
 398 spotted nitrocellulose membrane and detected using anti-His antibodies respectively. A clear
 399 binding of His-FT/TFL1 to PC was detected (**Figure 7B**) though these FT/TFL1 proteins
 400 have, not have or even in verse roles in flowering modulating.

402 Discussion

403 FT/TFL1 homologs exhibit both functional similarity and diversity across 404 various species

405 The plant PEBP family can be divided into three major clades, i.e. the *FT*-like, *MFT*-like and
406 *TFL1*-like clades. The first two act as promoters of flowering, whereas *TFL1*-like clade acts
407 as strong repressors of the response. Within the eight Rosaceae species, the *FT/TFL1*
408 homologs show high sequence identity (Supplementary Figure S1). Ectopic expression of
409 *PmTFL1*, *RoTFL1* and *FaTFL1* in tobacco extended the vegetative phase and resulted in a
410 significant delay in flowering. It is indicated that *TFL1* homologs play a conservative role in
411 controlling flowering time as previously reported for *AtTFL1*. However, most tobacco
412 overexpressing *PmFT* and *RoFT*, displayed extremely advanced flowering. Contrarily,
413 overexpression of *FaFT* did not promote flowering but, instead, caused slightly delayed by 1-
414 2 months than the wild-type (**Figure 2A, B; Table 1**). The results demonstrated a divergence
415 role of *FT* homologs between different species.

416 **FT homologs naturally evolved to have diverse roles in flowering time 417 control**

418 It has been reported that *AtFT* and *AtTFL1* may demonstrate interchangeable roles by
419 replacing a single amino acid (Hanzawa et al., 2005; Hou and Yang, 2009) or a larger protein
420 segment (Ahn et al., 2006; Pin et al., 2010). Tyr-85 in *AtFT* and His-88 in *AtTFL1* have been
421 identified as two key residues that determine the respective *FT* and *TFL1* functions (Hanzawa
422 et al., 2005). It is interesting that Tyr-85 and His-88 are conserved in all *FT* and *TFL1* proteins
423 from the eight Rosaceae species, respectively (Supplementary Figure S1). Sequence
424 comparison analyses showed that there are only 13 non-conserved substitutions between *Rosa*
425 *FT* (*RoFT*) and *Fragaria* *FT* (*FaFT*), but nevertheless the two genes demonstrated opposite
426 functions in controlling flowering time in transgenic plants (**Figure 2A**). In *Arabidopsis*,
427 protein segment B, in conjunction with the adjacent segment C, has been implicated as
428 essential for *FT*-like activity (Ahn et al., 2006). However, within this segment B we found
429 only one residue is different between *RoFT* and *FaFT*, i.e. Glu-139 in *RoFT* compared to Gly-
430 139 in *FaFT* and other *FT* homologs (Supplementary Figure S2). Thus, we suggest that
431 protein segment B is not critical to the activity of *FaFT* as a flowering repressor. Previous
432 study showed that *FT* protein is transported from the leaves, where it is synthesized, to the
433 shoot apex where it then interacts with FD, and so leads to the activation of floral meristem
434 identity genes *AP1*, *LFY* and *SOC1* (Abe et al., 2005; Wigge et al., 2005; Searle et al., 2006).
435 The expression of the endogenous genes *NtNFL*, *NtAP1* and *NtSOC1* were highly up-
436 regulated (49, 127 and 22 fold, respectively) in *35S::RoFT* transgenic tobacco line #1 (**Figure**
437 **4G-I**). The three site-directed mutants *RoFTmu1-3* acted as promoters of flowering in
438 transgenic tobacco lines and *ft-1* plants (**Figure 4A, 5E**), and resulted in the elevated
439 expression of the endogenous genes, the same as seen in response to *RoFT*. By contrast,
440 *RoFTmu4* and *RoFTmu5* demonstrated *TFL1*-like function in the flowering time, and the
441 expression of *NtNFL*, *NtAP1* and *NtSOC1* in tobacco transformed with these constructs was
442 about 2-fold higher than that of the control (**Figure 4G-I**). While we cannot rule out
443 complexities that might arise from co-suppression in specific constructs, considering the
444 consistent phenotypes between different ectopic transformants, it suggests that the phenotypes
445 were due to the over-expression of different site-mutated *RoFT*.

446 **Tyr-85 and Gln-140 amino acids are not sufficient for the promotion of 447 flowering by *FT* homologs**

448 *PhFT* from *Petunia hybrida* shares 71.0% and 54.4% identity with *AtFT* and *AtTFL1*,
449 respectively, and it encodes a typical *FT* residue Tyr-85 and an important IYN triplet motif
450 located in segment C. However, Lys-139 of *PhFT* differs from both counterparts from
451 *Arabidopsis* *FT* (Gln-140) and *TFL1* (Asp-144). Phylogenetic analysis placed *PhFT* in a
452 cluster with *FT*-like genes (**Figure 1C**), suggesting a putative *FT*-like function. Over-

453 expression of *PhFT* in tobacco did not promote early flowering (**Figure 2D, E**) instead,
454 strongly suppressed flowering of the transgenic tobacco. With a mutant *PhFTmu1* (K139Q),
455 ectopic expression of *PhFTmu1* in tobacco was found with late-flowering (**Figure 4C**). These
456 results of transgenic analysis were highly reminiscent of the *FT*-like repressor activity of
457 *BvFT1* in sugar beet (*Beta vulgaris* subsp. *vulgaris*), which exists alongside its antagonistic
458 paralog *BvFT2*. Although both of these *B. vulgaris* genes encode Tyr-85/Gln-140 residues and
459 the IYN triplet, they demonstrate a naturally evolved antagonistic function (Pin et al., 2010).
460 Similar findings have also been found in the *FT* gene family of tobacco and *Dimocarpus*
461 *longan* (Harig et al., 2012; Heller et al., 2014). Thus, the presence of Tyr-85, Gln-140 and
462 triplet IYN residues is not sufficient to indicate whether the *FT*-like proteins undertake the
463 role of flowering promoter or not. It has been reported that the three differing amino acids in
464 segment B, forming an external loop, are the major cause of the *BvFT1* and *BvFT2*
465 antagonistic function (Pin et al., 2010). However, analysis of the 14-amino-acid segment B of
466 *PhFT* by crystal structure analysis indicated a close resemblance to the tertiary structure of
467 *Arabidopsis* *FT*. Thus, further investigations are needed to elucidate the real reason why both
468 the *PhFT* and *PhFTmu1* proteins did not function to promote flowering in tobacco plants, as
469 predicted according to their key sequence traits.

470 **TFL1 substitution with key amino acids from FT did not promote flowering** 471 **in transgenic tobacco**

472 Previous reports described transgenic plants expressing the site-directed mutant *TFL1* genes
473 35S::*AtTFL1*-H88Y (Hanzawa et al., 2005) and 35S::*OnTFL1*-H85Y (Hou and Yang, 2009)
474 to show an early flowering phenotype, similar to that of *Arabidopsis* plants overexpressing
475 native *FT*. Here, we have described transgenic tobacco plants over-expressing *Rosa TFL1*
476 (*RoTFL1*) and *Fragaria TFL1* (*FaTFL1*) to show a late-flowering phenotype (**Figure 2H**).
477 Specific mutations were introduced into these Rosaceae genes, corresponding to the putative
478 key functional His-88 and Asp-144 residues of *AtTFL1*. However, these mutated genes did
479 not result in early-flowering phenotypes in the transgenic plants (**Table 3**), which is thereby
480 inconsistent with previous report. Based on our study in transgenic tobacco, key amino
481 substitution is not sufficient to promote flowering via *RoTFL1* and *FaTFL1* (**Figure 4D**).

482 **Site-directed mutations of IYN triplet motif resulted in loss of FT function**

483 According to a previous report (Ahn et al., 2006), exon 4 of *Arabidopsis* *FT* plays a critical
484 role in determining *FT/TFL1* function. The exon 4 sequence contains four segments, A-D, and
485 segments B and C are necessary for *FT*-like activity. These segments are also found in the
486 *TFL1* protein but, whereas the B and C sequences are highly conserved in many *FT* orthologs,
487 they appear to have diverged in proteins with *TFL1*-like activity (Ahn et al., 2006). In the
488 segment B encoded by *RoFT*, a single residue (Glu-139) is different from other *FT* homologs
489 (Supplementary Figure S2). Thus, considering that the consensus sequence of *FT* orthologs
490 contains a Gly residue at this corresponding site in the B segment and, despite this, *RoFT* still
491 functions as a flowering promoter, we suggest that the contrary action of the *FaFT* gene-
492 product as a floral repressor does not hinge on the sequence of segment B in exon 4. Among
493 our five *RoFT* mutants, three mutants outside of IYN triplet led to an early flowering
494 phenotype, similar to that mediated by over-expression of the unaltered *RoFT* gene. By
495 contrast, two mutants within the IYN triplet motif of segment C, were not effective in the
496 promotion of flowering and even to some extent, appeared to act similarly to a *TFL1*-like
497 floral repressor (**Figure 4A, 5A, 5E**).

498 **Interaction of FT homologs with FD protein and PC-binding ability is** 499 **independent to promote flowering**

Using yeast two-hybrid assays, Jang et al (2009) reported that *Arabidopsis* FT, but not TFL1, interacted with FD. However, Hanano and Goto (2011) used the BiFC technique to demonstrate that both TFL1 and FT can interact with FD within the plant cell nucleus (Hanano and Goto, 2011). In our yeast two-hybrid assays, FaTFL1 was found not to interact with FD, consistent with the findings of Jang et al (2009) but different with Abe et al (2005). However, we also found that PhFT, in spite of having high sequence similarity to FT, showed the same interaction pattern as FaTFL1. Our system was able to verify that native *Arabidopsis* FT interacted with FD. RoFT and the five corresponding point mutated protein forms were all shown to interact with AtFD in a similar way to the native *Arabidopsis* FT, which is also strongly supported by our BiFC system (**Figure 6**). In addition, ectopic overexpression of AtFD led to 2-3-months early-flowering in tobacco (Supplementary Figure S4, Supplementary Table S8), which showed that the AtFD is functionally active in tobacco as is the case of 35S::AtFD in *Arabidopsis* (Abe et al., 2005; Wigge et al., 2005). Since over-expression of the *RoFTmu4* did not promote flowering in tobacco or *Arabidopsis*, we conclude that the physical interaction of FT homologs with the FD protein is not sufficient to bring about the promotion of flowering. These results also indicate that the substitution of a single amino acid residue of RoFT does not necessarily have a major impact on its interaction with FD but may, nevertheless, change its role in the control of flowering. Other interaction partners specific to FT or TFL1 are likely to exist, and this is supported by other studies (Jang et al, 2009; Taoka et al., 2011; Ho and Weigel, 2014). On the other hand, the diversity of interaction with AtFD in TFL1 homologs, verified by yeast two-hybrid and BiFC system, also show no correlation to their roles in flowering delaying. Though FT/TFL1 share a similar 3D structure with animal PEBP with an anion binding pocket, neither FT nor TFL1 were shown to bind any phospholipids *in vivo*. In another study, point mutation of the *Arabidopsis* FT at Asp71 located in the deep pocket did not affect FT activity (Ho and Weigel, 2014). So the significance of the pocket is unclear.

It has been reported that FT binds the phospholipid phosphatidylcholine (PC), a component of cellular membranes whose higher level accelerates flowering. Two models have been proposed to explain the effect of PC on flowering control (Nakamura et al., 2014). As a component of the nuclear membrane, PC may attract free FT from the cytosol into nucleus to promote flowering. Alternatively, PC-containing vesicles could help trafficking of FT to FD. Our FT-lipid assay result shows that whether they promote flowering or not, all FT/TFL1 homologs have the lipid-binding properties (**Figure 7B**). Thus, it is also deduced that lipid-binding and flowering promotion were two independent events. Considering TFL1 homologs have opposite function in controlling flowering, the PC-binding ability may imply other functions such as in mobile signaling. The *TFL1* gene is transcribed in the central region of the SAM, and the protein spreads throughout the IM (dose not reach FM). By contrast, FT is produced in leaves and then is moved into SAMs (Bernier and Périlleux, 2005; Conti and Bradley, 2007; Wickland and Hanzawa, 2015). TFL1 was reported to play a role in endomembrane trafficking to protein storage vacuoles (PSVs) (Sohn et al., 2007). In addition to the fact that TFL1 protein is located in both the nucleus and cytoplasm, thus, TFL1 maybe shuttle FD from nuclei to PSVs, in nuclei where FT recruits FD, to block FD-dependent transcription occurs (Hanano and Goto, 2011). It also implies the TFL1 functions obviously in protein trafficking to PSVs from that the PC binding of His-TFL1 looks stronger than His-FT.

Collectively, beside description of the functional divergences in many FT/TFL1 homologs, our data have also shown that many novel amino acids change can switch FT-like activity to TFL1-like activity. On the other hand, it is also verified that the divergence of flowering time modulating by FT/TFL1 homologs is independent to its interaction and binding activities.

549 **Author contribution**

550 GN and ZW designed the experiments and drafted the manuscript. RY, UD, JM, YZ, JL and
551 YS participated in the coordination of the experiments. GN, JZ and MB thoroughly revised
552 the manuscript and finalized the manuscript. All the authors read and approved the
553 manuscript.

554 **Acknowledgments**

555 This work was supported by grants from the National Natural Science Foundation of China
556 (no. 31572160) and the Fundamental Research Funds for the Central Universities
557 (2662015PY112). We thank all the colleagues in the lab for constructive discussion and
558 technical support. We are also grateful to Dr. Alex C. McCormac for critical editing of the
559 manuscript.

560

561 **Supplemental Data**

562 Supplementary Figure S1. Alignment of amino acid sequences of *FT/TFL1* homologs of eight Rosaceae
563 species.

564 Supplementary Figure S2. Alignment of amino acid sequences of *FT/TFL1* homologs.

565 Supplementary Figure S3. Transformed yeast cells were grown on SD/-Leu-Trp selection medium in Yeast
566 two-hybrid analysis.

567 Supplementary Figure S4. Phenotype of transgenic tobacco plants harboring *Arabidopsis* FD (AtFD).

568 Supplementary Table S1. Gene specific primers used in FPNI-PCR.

569 Supplementary Table S2. The universal primers used in FPNI-PCR.

570 Supplementary Table S3. Gene specific primers used to isolate complete *FT/TFL1* coding sequences.

571 Supplementary Table S4. Gene specific primers used to construct expression plasmid.

572 Supplementary Table S5. Gene specific primers used for RT-PCR analysis.

573 Supplementary Table S6. Gene specific primers used for qRT-PCR analysis.

574 Supplementary Table S7. Gene specific primers used to construct yeast two-hybrid and BiFC vectors.

575 Supplementary Table S8. Phenotypic analysis of transgenic tobacco plants harboring *Arabidopsis* FD
576 (AtFD).

577

578 **References**

579 Abe, M., Kobayashi, Y., Yamamoto, S., Daimon, Y., Yamaguchi, A., Ikeda, Y., et al. (2005). FD, a bZIP
580 protein mediating signals from the floral pathway integrator FT at the shoot apex. *Science* 309: 1052–
581 1056. doi: 10.1126/science.1115983

582 Ahn, J. H., Miller, D., Winter, V. J., Banfield, M. J., Lee, J. H., Yoo, S. Y., et al. (2006). A divergent external
583 loop confers antagonistic activity on floral regulators FT and TFL1. *EMBO J.* 25: 605–614. doi:
584 10.1038/sj.emboj.7600950

585 Arnold, K., Bordoli, L., Kopp, J., and Schwede, T. (2006). The SWISS-MODEL Workspace: A web-based
586 environment for protein structure homology modeling. doi: 10.1093/bioinformatics/bti770

587 Banfield, M. J., Barker, J. J., Perry, A. C., and Brady, R. L. (1998). Function from structure? The crystal
588 structure of human phosphatidylethanolamine-binding protein suggests a role in membrane signal
589 transduction. *Structure* 6: 1245–1254. doi: 10.1016/S0969-2126(98)00125-7

590 Banfield, M. J., and Brady, R. L. (2000). The structure of *Antirrhinum centroradialis* protein (CEN)
591 suggests a role as a kinase regulator. *J. Mol. Biol.* 297: 1159–1170.

- 592 Benlloch, R., Kim, M.C., Sayou, C., Thevenon, E., Parcy, F., and Nilsson, O. (2011). Integrating long-day
593 flowering signals: a LEAFY binding site is essential for proper photoperiodic activation of
594 APETALA1. *Plant J.* 67:1094–1102. doi: 10.1111/j.1365-313X.2011.04660.x
- 595 Bernier, G., and Périlleux, C. (2005). A physiological overview of the genetics of flowering time
596 control. *Plant Biotechnology Journal*, 3(1): 3-16. doi: 10.1111/j.1467-7652.2004.00114.x
- 597 Bradley, D. J., Carpenter, R., Copsey, L., Vincent, C., Rothstein, S., and Coen, E. S. (1996). Control of
598 inflorescence architecture in *Antirrhinum*. *Nature* 379:791–797. doi: 10.1038/379791a0
- 599 Bradley, D. J., Ratcliffe, O. J., Vincent, C., Carpenter, R., and Coen, E. S. (1997). Inflorescence
600 commitment and architecture in *Arabidopsis*. *Science* 275: 80–83. doi: 10.1126/science.275.5296.80
- 601 Chautard, H., Jacquet, M., Schoentgen, F., Bureaud, N., and Benedetti, H. (2004). Tfs1p, a member of the
602 PEBP family, inhibits the Ira2p but not the Ira1p Ras GTPase-activating protein in *Saccharomyces*
603 *cerevisiae*. *Eukaryotic Cell* 3: 459–470. doi: 10.1128/EC.3.2.459-470.2004
- 604 Coelho, C. P., Minow, M. A., Chalfun-Júnior, A., and Colasanti, J. (2014). Putative sugarcane FT/TFL1
605 genes delay flowering time and alter reproductive architecture in *Arabidopsis*. *Front. Plant Sci.* 5: 221.
606 doi: 10.3389/fpls.2014.00221
- 607 Conti, L., and Bradley, D. (2007). TERMINAL FLOWER1 is a mobile signal controlling *Arabidopsis*
608 architecture. *Plant Cell* 19: 767–778. doi: 10.1105/tpc.106.049767
- 609 Corbesier, L., Vincent, C., Jang, S., Fornara, F., Fan, Q., Searle I., et al. (2007). FT protein movement
610 contributes to long-distance signaling in floral induction of *Arabidopsis*. *Science* 316: 1030–1033. doi:
611 10.1126/science.1141752
- 612 Fu, Z., Smith, P. C., Zhang, L., Rubin, M. A., Dunn, R. L., Yao, Z., and Keller, E. T. (2003). Effects of Raf
613 Kinase inhibitor protein expression on suppression of prostate cancer metastasis. *J. Natl. Cancer Inst.*
614 95: 878–889. doi: 10.1093/jnci/95.12.878
- 615 Gibson, D. G., Young L., Chuang, R. Y., Venter, J. C., Hutchison, C. A., and Smith, H. O. (2009) Enzymatic
616 assembly of DNA molecules up to several hundred kilobases. *Nature methods* 6(5): 343-345.
617 doi:10.1038/nmeth.1318
- 618 Grandy, D. K., Hanneman, E., Bunzow, J., Shih, M., Machida, C. A., Bidlack J. M., and Civelli, O. (1990).
619 Purification, cloning, and tissue distribution of a 23-kD rat protein isolated by morphine affinity
620 chromatography. *Mol. Endocrinol.* 4(9): 1370-1376. doi: http://dx.doi.org/10.1210/mend-4-9-1370
- 621 Hanano, S., and Goto, K. (2011). *Arabidopsis* TERMINAL FLOWER1 is involved in the regulation of
622 flowering time and inflorescence development through transcriptional repression. *Plant Cell* 23 (9) :
623 3172-3184. doi: 10.1105/tpc.111.088641
- 624 Hanzawa, Y., Money, T., and Bradley, D. (2005). A single amino acid converts a repressor to an activator of
625 flowering. *Proc. Natl. Acad. Sci. USA* 102: 7748-7753. doi: 10.1073/pnas.0500932102
- 626 Harig, L., Beinecke, F. A., Oltmanns, J., Muth, J., Muller, O., Ruping, B., and Noll, G. A. (2012). Proteins
627 from the FLOWERING LOCUS T-like subclade of the PEBP family act antagonistically to regulate
628 floral initiation in tobacco. *Plant J.* 72: 908–921. doi: 10.1111/j.1365-313X.2012.05125.x
- 629 Heller, W. P., Ying, Z., Davenport, T. L., Keith, L. M., and Matsumoto, T. K. (2014). Identification of
630 members of the Dimocarpus Longan Flowering Locus T gene family with divergent functions in
631 flowering. *Tropical Plant Biol.* 7:19-29. doi: 10.1007/s12042-013-9134-0
- 632 Hengst, U., Albrecht, H., Hess, D., and Monard, D. (2001). The Phosphatidylethanolamine-binding protein
633 is the prototype of a novel family of serine protease inhibitors. *J. Biol. Chem.* 276: 535–540. doi:
634 10.1074/jbc.M002524200
- 635 Ho, S. N., Hunt, H. D., Horton, R. M., Pullen, J. K., and Pease, L. R. (1989). Site-directed mutagenesis by
636 overlap extension using the polymerase chain reaction. *Gene* 77(1): 51-59. doi: 10.1016/0378-
637 1119(89)90358-2
- 638 Ho, W. W., and Weigel, D. (2014). Structural features determining flower-promoting activity of *Arabidopsis*
639 FLOWERING LOCUS T. *Plant cell* 26: 552-564. doi: 10.1105/tpc.113.115220

- 640 Hou, C. J., and Yang, C. H. (2009). Functional Analysis of FT and TFL1 orthologs from Orchid (*Oncidium*
641 Gower Ramsey) that regulate the vegetative to reproductive transition. *Plant and cell Physiology* 50(8):
642 1544–1557. doi: 10.1093/pcp/pcp099
- 643 Hu, C. G., Honda, C., Kita, M., Zhang, Z. L., and Tsuda, T. T. (2002). A simple protocol for RNA isolation
644 from fruit trees containing high levels of polysaccharides and polyphenol compounds. *Plant*
645 *Molecular Biology Reporter* 20: 69. doi: 10.1007/BF02801935
- 646 Imamura, T., Nakatsuka, T., Higuchi, A., Nishihara, M., and Takahashi, H. (2011). The gentian orthologs of
647 the FT/TFL1 gene family control floral initiation in *Gentiana*. *Plant and cell physiology* 52(6): 1031-
648 1041. doi: 10.1093/pcp/pcr055
- 649 Jang, S., Torti, S., and Coupland, G. (2009). Genetic and spatial interactions between FT, TSF and SVP
650 during the early stages of floral induction in *Arabidopsis*. *Plant J.* 60: 614–625. doi: 10.1111/j.1365-
651 313X.2009.03986.x
- 652 Kardailsky, I., Shukla, V. K., Ahn, J. H., Dagenais, N., Christensen, S. K., Nguyen, J. T., and Weigel, D.
653 (1999). Activation tagging of the floral inducer FT. *Science* 286: 1962–1965. doi:
654 10.1126/science.286.5446.1962
- 655 Kobayashi, Y., Kaya, H., Goto, K., Iwabuchi, M., and Araki, T. (1999). A pair of related genes with
656 antagonistic roles in mediating flowering signals. *Science* 286: 1960–1962. doi:
657 10.1126/science.286.5446.1960
- 658 Kobayashi, Y., and Weigel, D. (2007). Move on up, it's time for change-Mobile signals controlling
659 photoperiod-dependent flowering. *Genes Dev.* 21: 2371–2384. doi: 10.1101/gad.1589007
- 660 Li, X., Ning, G., Han, X., Liu, C., and Bao, M. (2015). The identification of novel PMADS3 interacting
661 proteins indicates a role in post-transcriptional control. *Gene* 564: 87-95. doi:
662 10.1016/j.gene.2015.03.052
- 663 Mutasa-Gätgens, E., and Hedden, P. (2009). Gibberellin as a factor in floral regulatory networks. *Journal*
664 *of Experimental Botany* 60: 1979–1989. doi: 10.1093/jxb/erp040
- 665 Nakamura, Y., Andrés, F., Kanehara, K., Liu, Y.C., Dörmann, P., and Coupland, G. (2014). *Arabidopsis*
666 florigen FT binds to diurnally oscillating phospholipids that accelerate flowering. *Nature*
667 *Communication* 5: 3553. doi: 10.1038/ncomms4553
- 668 Ning, G., Xiao, X., Lv, H., Li, X., Zuo, Y., and Bao, M. (2012). Shortening tobacco life cycle accelerates
669 functional gene identification in genomic research. *Plant Biology* 14(6):934-943. doi:10.1111/j.1438-
670 8677.2012.00571.x
- 671 Notaguchi, M., Abe, M., Kimura, T., Daimon, Y., Kobayashi, T., Yamaguchi, A., and Araki, T. (2008).
672 Long-distance, graft-transmissible action of *Arabidopsis* FLOWERING LOCUS T protein to promote
673 flowering. *Plant and cell physiology* 49(11): 1645-1658. . doi: 10.1093/pcp/pcn154
- 674 Ohshima, S., Murata, M., Sakamoto, W., Ogura, Y., and Motoyoshi, F. (1997). Cloning and molecular
675 analysis of the *Arabidopsis* gene Terminal Flower 1. *Mol. Gen. Genet.* 254: 186–194. doi:
676 10.1007/s004380050407
- 677 Pettersen, E. F., Goddard, T. D., Huang, C. C., Couch, G. S., Greenblatt, D. M., Meng, E. C., and Ferrin,
678 T.E. (2004). UCSF Chimera—A visualization system for exploratory research and analysis. *Journal of*
679 *Computational Chemistry* 25: 1605–1612. doi: 10.1002/jcc.20084
- 680 Pin, P. A., Benlloch, R., Bonnet, D., Wremerth-Weich, E., Kraft, T., Gielen, J. J., and Nilsson, O. (2010). An
681 antagonistic pair of FT homologs mediates the control of flowering time in sugar beet. *Science* 330:
682 1397–1400. doi: 10.1126/science.1197004
- 683 Pnueli, L., Carmel-Goren, L., Hareven, D., Gutfinger, T., Alvarez, J., Ganal, M., and Lifschitz, E. (1998).
684 The SELF-PRUNING gene of tomato regulates vegetative to reproductive switching of sympodial
685 meristems and is the ortholog of CEN and TFL1. *Development* 125: 1979–1989.
- 686 Pnueli, L., Gutfinger, T., Hareven, D., Ben-Naim, O., Ron, N., Adir, N., and Lifschitz, E. (2001). Tomato
687 SP-Interacting Proteins Define a Conserved Signaling System That Regulates Shoot Architecture and
688 Flowering. *Plant Cell* 13: 2687–2702. doi: 10.1105/tpc.13.12.2687

- 689 Searle, I., He, Y., Turck, F., Vincent, C., Fornara, F., Kröber, S., and Coupland, G. (2006). The transcription
690 factor FLC confers a flowering response to vernalization by repressing meristem competence and
691 systemic signaling in *Arabidopsis*. *Genes Dev.* 20: 898-912. doi: 10.1101/gad.373506
- 692 Serre, L., Vallee, B., Bureaud, N., Schoentgen, F., and Zelwer, C. (1998). Crystal structure of the
693 phosphatidylethanolamine-binding protein from bovine brain: a novel structural class of phospholipid-
694 binding proteins. *Structure* 6: 1255-1265. doi: 10.1016/S0969-2126(98)00126-9
- 695 Simister, P. C., Banfield, M. J., and Brady, R. L. (2002). The crystal structure of PEBP-2, a homologue of
696 the PEBP/RKIP family. *Acta Crystallogr D* 58: 1077-1080. doi: 10.1107/S090744490200522X
- 697 Smykal, P., Gennen, J., Bodt, S., Ranganath, V., and Melzer, S. (2007) Flowering of strict photoperiodic
698 Nicotiana varieties in non-inductive conditions by transgenic approaches. *Plant Mol Biol.* 65: 233-242.
699 doi: 10.1007/s11103-007-9211-6
- 700 Sohn, E. J., Rojas-Pierce, M., Pan, S., Carter, C., Serrano-Mislata, A., Madueno, F., Rojo, E., Surpin, M.,
701 Raikhel, N.V. (2007). The shoot meristem identity gene TFL1 is involved in flower development and
702 trafficking to the protein storage vacuole. *Proc. Natl. Acad. Sci. USA.* 104: 18801-18806. doi:
703 10.1073/pnas.0708236104
- 704 Stevenson, J. M., Perera, I. Y., and Boss, W. F. (1998) A Phosphatidylinositol 4-Kinase Pleckstrin
705 Homology Domain That Binds Phosphatidylinositol 4-Monophosphate. *Journal of Biological
706 Chemistry* 273(35): 22761-22767. doi: 10.1074/jbc.273.35.22761
- 707 Tamaki, S., Matsuo, S., Wong, H. L., Yokoi, S., and Shimamoto, K. (2007). Hd3a protein is a mobile
708 flowering signal in rice. *Science* 316: 1033-1036. doi: 10.1126/science.1141753
- 709 Tamura, K., Peterson, D., Peterson, N., Stecher, G., Nei, M., and Kumar, S. (2011). MEGA5, molecular
710 evolutionary genetics analysis using maximum likelihood, evolutionary distance, and maximum
711 parsimony methods. *Mol. Biol. Evol.* 28 (10): 2731-2739. doi: 10.1093/molbev/msr121
- 712 Taoka, K., Ohki, I., Tsuji, H., Furuita, K., Hayashi, K., Yanase, T., and Ogaki, Y. (2011). 14-3-3 proteins act
713 as intracellular receptors for rice Hd3a florigen. *Nature* 476: 332-335. doi:10.1038/nature10272
- 714 Turnbull, C. (2011). Long-distance regulation of flowering time. *Journal of Experimental Botany* 62: 4399-
715 4413. doi: 10.1093/jxb/err191
- 716 Wagner, D. (2016). Making Flowers at the Right Time. *Developmental cell* 37(3): 208-210. doi:
717 10.1016/j.devcel.2016.04.021
- 718 Wang, R. H., Albani, M. C., Vincent, C., Bergonzi, S., Luan, M., Bai, Y., and Coupland, G. (2011a). Aa
719 TFL1 confers an age-dependent response to vernalization in perennial *Arabis alpina*. *Plant Cell* 4(23):
720 1307-1321. doi:10.1105/tpc.111.083451
- 721 Wang, Z., Ye, S. F., Li, J. J., Zheng, B., Bao, M. Z., and Ning, G. G. (2011). Fusion primer and nested
722 integrated PCR (FPNI-PCR): a new high-efficiency strategy for rapid chromosome walking or
723 flanking sequence cloning. *BMC Biotechnology* 11: 109. doi: 10.1186/1472-6750-11-109
- 724 Wickland, D. P., and Hanzawa, Y. (2015). The FLOWERING LOCUS T/TERMINAL FLOWER 1 Gene
725 Family: Functional Evolution and Molecular Mechanisms. *Molecular Plant* 8: 983-997. doi:
726 10.1016/j.molp.2015.01.007
- 727 Wigge, P. A., Kim, M. C., Jaeger, K. E., Busch, W., Schmid, M., Lohmann, J. U., and Weigel, D. (2005).
728 Integration of spatial and temporal information during floral induction in *Arabidopsis*. *Science* 309:
729 1056-1059. doi: 10.1126/science.1114358
- 730 Wolabu, T. W., Zhang, F., Niu, L., Kalve, S., Bhatnagar-Mathur, P., Muszynski, M. G., and Tadege, M.
731 (2016) Three FLOWERING LOCUS T-like genes function as potential florigens and mediate
732 photoperiod response in sorghum. *New Phytologist* 210: 946-959. doi: 10.1111/nph.13834
- 733 Xing, W., Wang, Z., Wang, X. Q., Bao, M. Z., and Ning G.G. (2014). Over-expression of an FT homolog
734 from *Prunus mume* reduces juvenile phase and induces early flowering in rugosa rose. *Scientia
735 Horticulturae* 172: 68-72. doi: 10.1016/j.scienta.2014.03.050
- 736 Zhang, J., Yan, G., Wen, Z., An, Y., Singer, S., and Liu, Z. (2014) Two tobacco AP1-like gene promoters
737 drive highly specific, tightly regulated and unique expression patterns during floral transition,

738 initiation and development. *Planta* 239: 469-478. doi: 10.1007/s00425-013-1995-9

739

740 Figure legends

741 **Figure 1.** Gene structures and phylogenetic analysis of the *FT/TFL1* homologs. Gene structures of: (A) *FT*
742 and (B) *TFL1* homologs isolated from eight Rosaceae species including *Prunus mume* (*PmFT*), *Rosa*
743 (*RoFT*), *Fragaria* (*FaFT*), *Photinia* (*PsFT*), *Pyracantha* (*PfFT*), *Spiraea* (*ScFT*), *Prunus persica* (*PpFT*);
744 *Prunus mume* (*PmTFL1*), *Rosa* (*RoTFL1*), *Fragaria* (*FaTFL1*), *Photinia* (*PsTFL1*), *Pyracantha* (*PfTFL1*),
745 *Spiraea* (*ScTFL1*), *Prunus yedoensis* (*PyTFL1*). Boxes indicate exons and lines indicate introns; the
746 numbers represent their corresponding lengths (bp). (C) Phylogenetic analysis of the *FT/TFL1* homologs
747 from different plant species. Under-lined genes represent *FT/TFL1* homologs isolated from Rosaceae
748 species and asterisks represent gene sequences used for function identification in this study.

749 **Figure 2.** Phenotypic analysis of transgenic tobacco plants harboring different *FT/TFL1* homologs from
750 various species. (A) From left to right are wild-type, and transgenic plants harboring *FaFT* and *RoFT*,
751 respectively, after growth for 1 month. (B) Tobacco plant harboring 35S::*PmFT* and showing visible flower
752 bud in culture box. (C) RT-PCR analysis to confirm the *FT* transgenic lines. (D-E) Transgenic tobacco
753 plants harboring *PhFT* showing normal growth and no early flowering phenotype after growth for 1.5
754 months and 5 months, respectively. (F) RT-PCR analysis to confirm *PhFT* transgenic lines. (G) RT-PCR
755 analysis to confirm *FaTFL1* and *RoTFL1* transgenic lines. (H) Transgenic tobacco plants harboring
756 *FaTFL1* and *RoTFL1* after growth for 13 months.

757 **Figure 3.** Crystal structures of FT and TFL1 and maps of point mutated residues. (A) Cartoon diagrams of
758 four FT or TFL1 homologs. The red highlighted residues show the corresponding mutated points that were
759 substituted for use in transgenic experiments. The protein pairs: *RoFT/PhFT* and *RoTFL1/FaTFL1* present
760 highly similar crystal structures to each other. (B) Diagram mapping the corresponding mutated amino acid
761 residues of FT or TFL1 homologs. (C) Schematic map of the T-DNA region (vector pMOG22) used to
762 perform the transgenic experiments.

763 **Figure 4.** Phenotypic analysis of transgenic tobacco plants harboring different *FT/TFL1* homologs. (A)
764 From left to right, 35S::*RoFTmu1-5*, wild-type and 35S::*RoFT* plants, respectively, after growth for 45
765 days. (B) RT-PCR analysis to confirm the transgenic lines. (C) From left to right are wild-type, and
766 transgenic plants harboring *PhFTmu1* (2 lines) after growth for 3 months. (D) From left to right are wild-
767 type, transgenic plants harboring *RoTFL1mu1*, *RoTFL1mu2* and *FaTFL1mu1* after growth for 4 months.
768 (E-F) RT-PCR analysis to confirm the transgenic lines. (G-I) qRT-PCR analysis of endogenous flowering
769 genes in 45-day-old seedlings of transgenic and wild-type tobacco. The transcript levels of: (G) *NtNFL*, (H)
770 *NtAPI* and (I) *NtSOC1* in different transgenic tobacco lines harboring various point mutations of *FT*. In this
771 analysis, *NtEF1α* was used as a reference transcript. Three biological replications were performed
772 randomly for each transgenic line.

773 **Figure 5.** Phenotypic analysis of ectopically expressing mutated *RoFT* transcripts in the Col and *ft-1*
774 Background. (A) 25-day-old 35S::*Roftmu3* (A116S) plant (centre) flowering 20 days after germination
775 which was earlier than wild-type Col (left) and 35S::*Roftmu4* (Y153C) (right). Leaf number (B) and time
776 from seed to bolting (C) of wild-type Col and transgenic *Arabidopsis* plants under LD (16-h-light/8-h-dark)
777 conditions. RL, rosette leaves; CL, cauline leaves. (D) qRT-PCR analysis of endogenous flowering genes
778 *AtAPI* in 3-week-old seedlings of wild-type Col and transgenic *Arabidopsis* plants. *AtEF1α* was used as a
779 reference transcript. Three biological replications were performed randomly for each transgenic line. (E)
780 From left to right, 35S::*RoFTmu1-5*, *ft-1*, 35S::*RoFT* and *Ler*. 35S::*RoFT* and 35S::*RoFTmu1-3* plants
781 flowering 25 days after germination which were earlier than *ft-1* mutant. (F) RT-PCR analysis to confirm
782 the transgenic lines. Leaf number (G) and time from seed to bolting (H) of *ft-1* and transgenic *Arabidopsis*
783 plants under LD (16-h-light/8-h-dark) conditions. Asterisks show that the values are significantly different
784 between the transgenic lines and the control (*P < 0.05; **P < 0.01; ***P < 0.001).

785 **Figure 6.** Interaction of FT/TFL1 and AtFD proteins. (A) Yeast two-hybrid analysis to study the interaction
786 among different FT/TFL1 homologs. Transformed yeast cells (10^3 or 10^4 diluted) were grown on selection
787 medium containing X-a-Gal. (B) BiFC analysis of protein interactions between different FT/TFL1
788 homologs and AtFD in *N. benthamiana* leaf epidermis cells. YFP, YFP fluorescence; DAPI, DAPI
789 fluorescence; BF, bright field image; Merged, merge of YFP, DAPI and BF. The AtFT with AtFD
790 interaction was used as a positive control. Bars=10 μm.

791 **Figure 7.** FT proteins binding to phosphatidylcholine (PC). (A) His-FT/TFL1 purified proteins on SDS-
792 PAGE Gel. M, Protein Marker; 1-11, His-AtFT, His-RoFT, His-RoFTmu2, His-RoFTmu3, His-RoFTmu4,
793 His-RoFTmu5, His-PhFT, His-AtTFL1, His-RoTFL1, His-FaTFL1, His-only. (B) Various His-FT/TFL1
794 proteins binding to di 18:1 PC on the membrane. The His-AtFT and His-only with PC binding was used as
795 a positive and negative control, respectively.

796

797

Figure 01.TIF

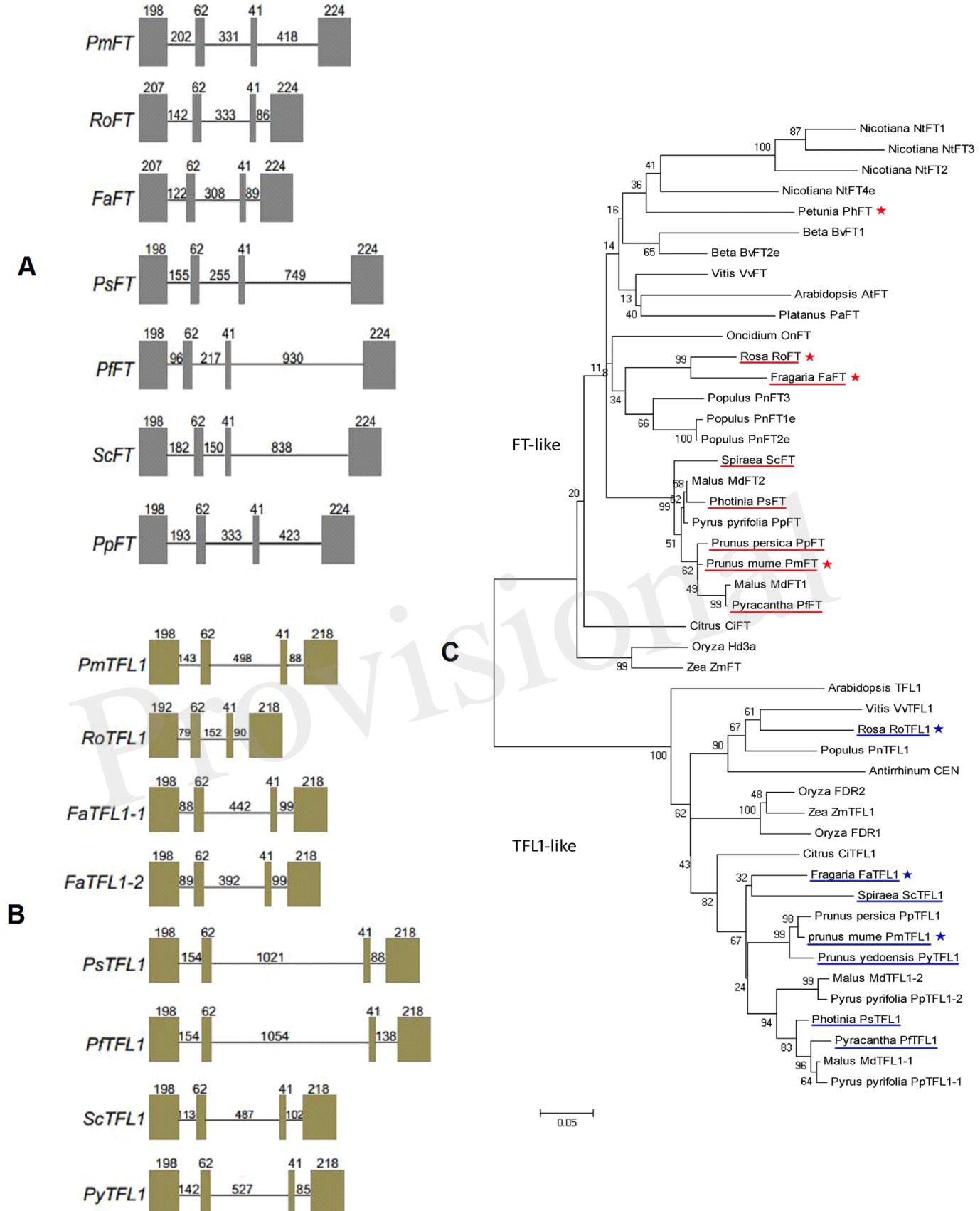


Figure 02.TIF

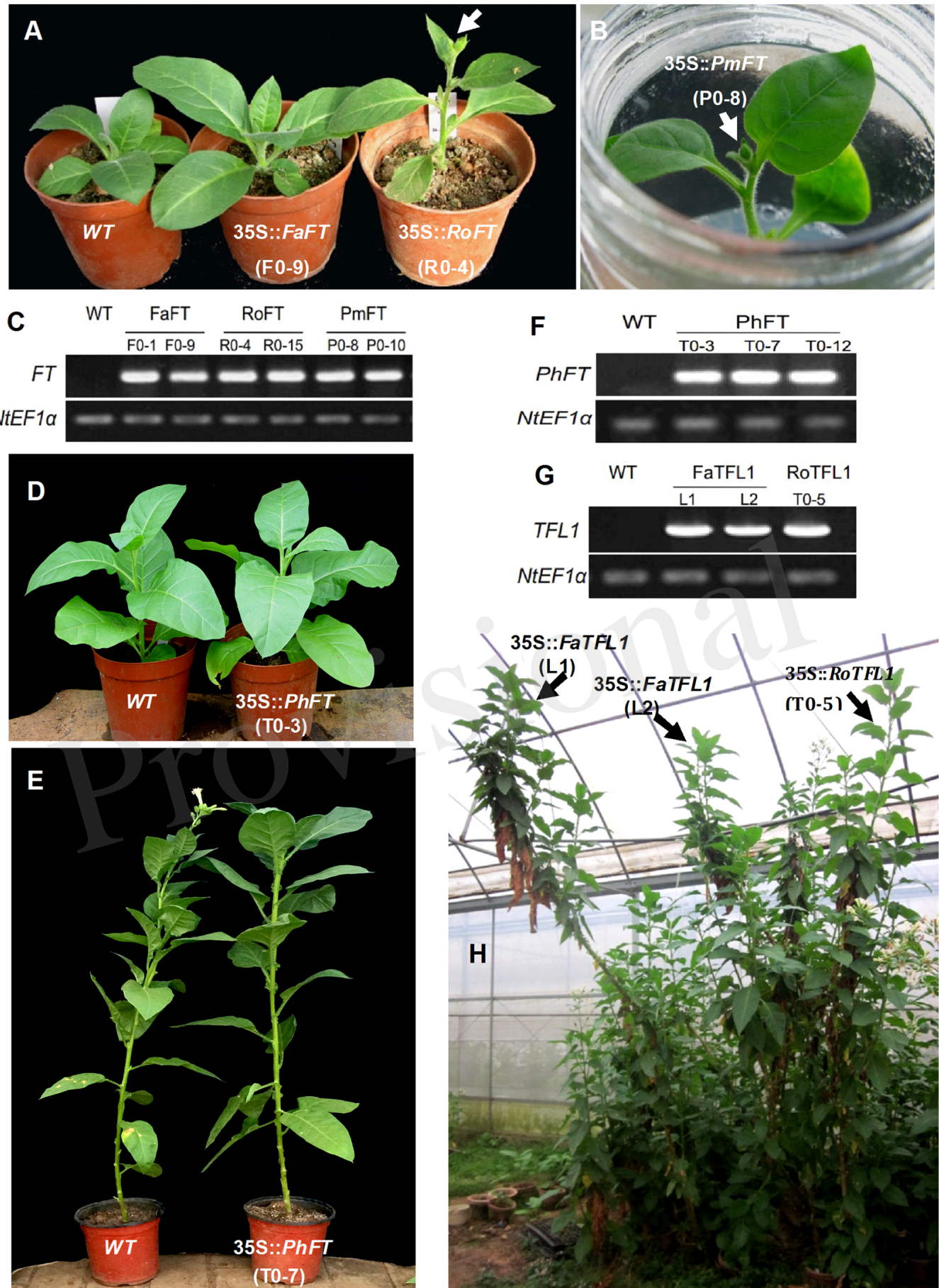


Figure 03.TIF

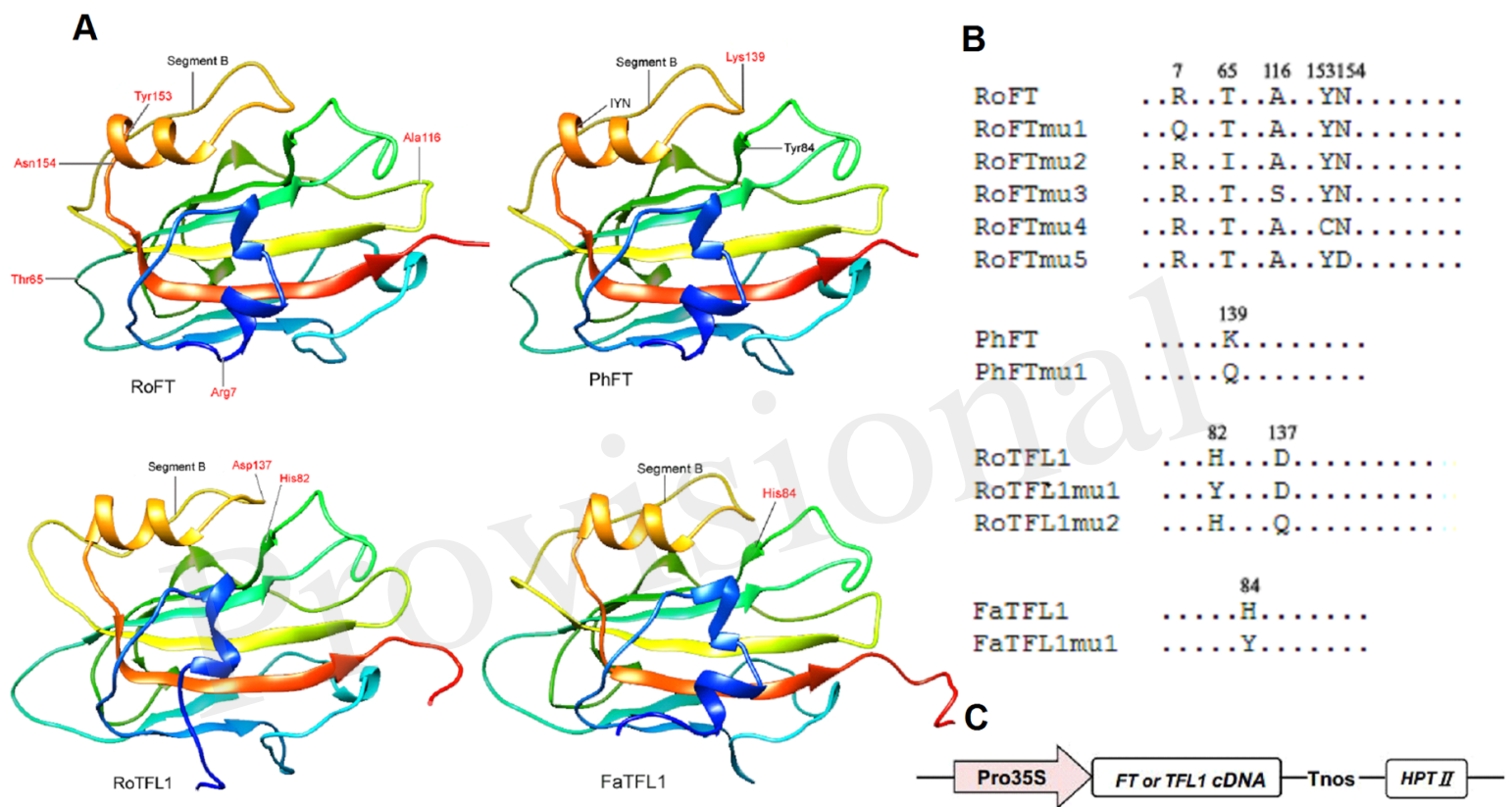


Figure 04.TIF

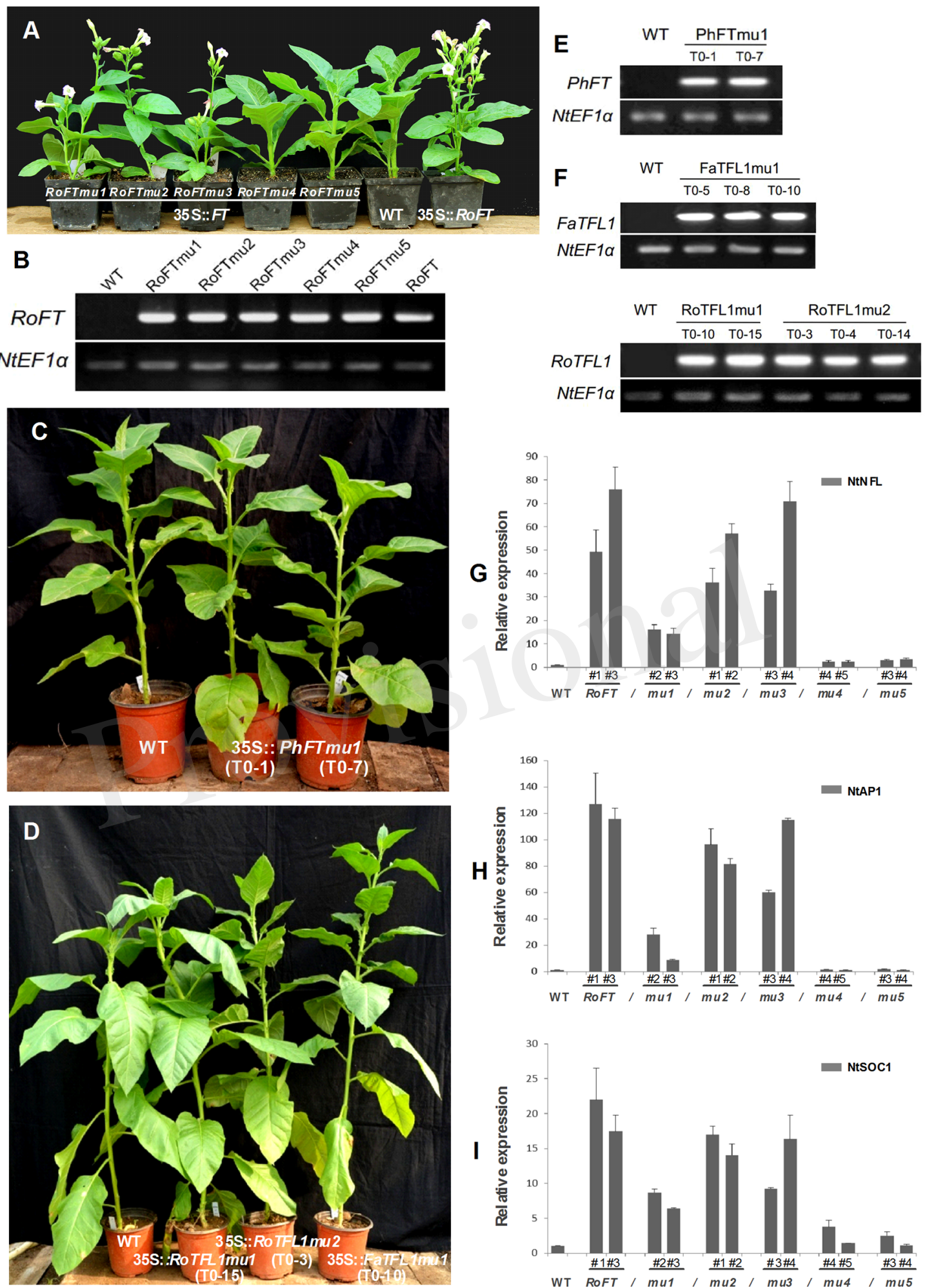


Figure 06.TIF

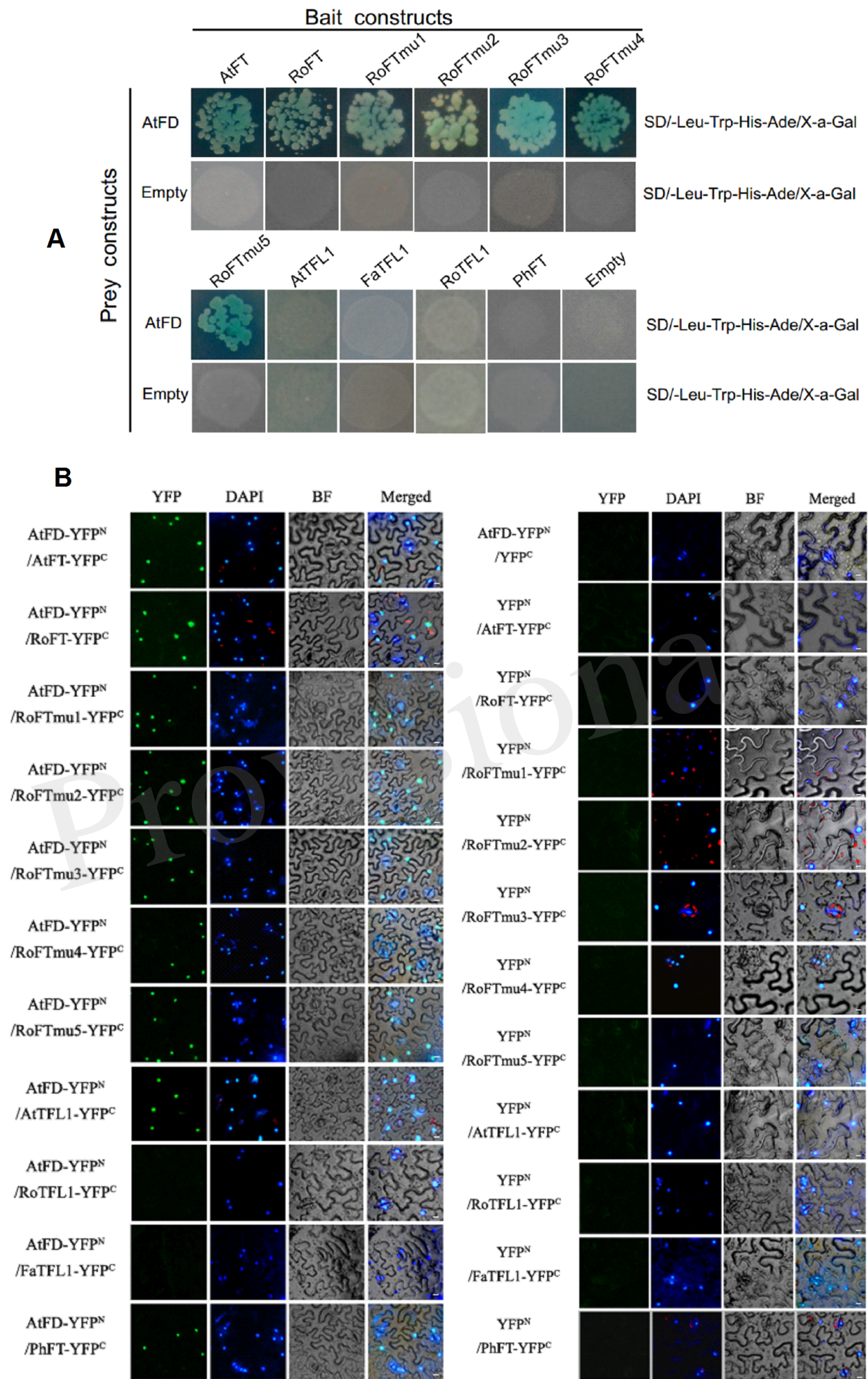
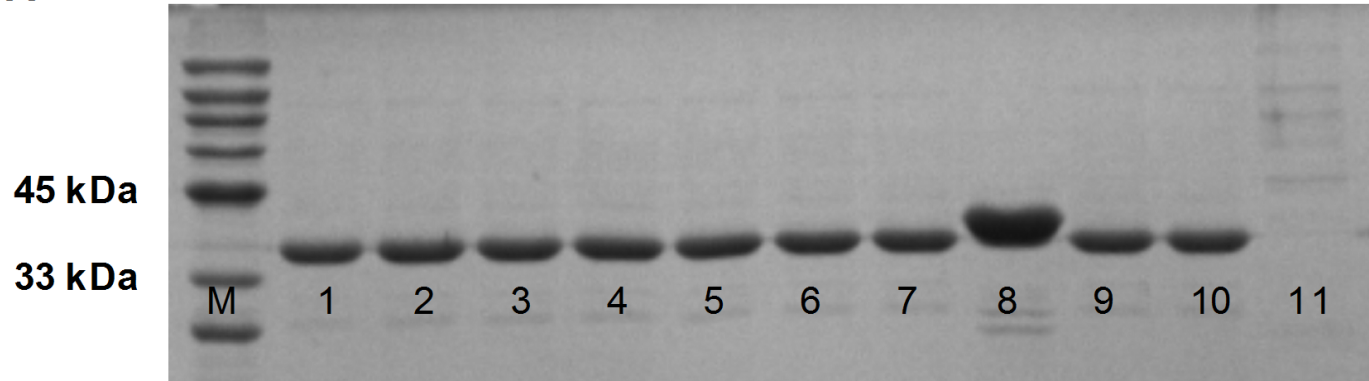


Figure 07.TIF

A



B

